NASA/TM—2013-216613

Comparison of Hyperthermal Ground Laboratory Atomic Oxygen Erosion Yields With Those in Low Earth Orbit

Bruce A. Banks
Science Application International Corporation, Cleveland, Ohio

Grace C. Dill and Ryan J. Loftus
Alphaport, Incorporated, Cleveland, Ohio

Kim K. de Groh and Sharon K. Miller
Glenn Research Center, Cleveland, Ohio

December 2013

NASA STI Program . . . in Profile

Since its founding, NASA has been dedicated to the advancement of aeronautics and space science. The NASA Scientific and Technical Information (STI) program plays a key part in helping NASA maintain this important role.

The NASA STI Program operates under the auspices of the Agency Chief Information Officer. It collects, organizes, provides for archiving, and disseminates NASA's STI. The NASA STI program provides access to the NASA Aeronautics and Space Database and its public interface, the NASA Technical Reports Server, thus providing one of the largest collections of aeronautical and space science STI in the world. Results are published in both non-NASA channels and by NASA in the NASA STI Report Series, which includes the following report types:

- TECHNICAL PUBLICATION. Reports of completed research or a major significant phase of research that present the results of NASA programs and include extensive data or theoretical analysis. Includes compilations of significant scientific and technical data and information deemed to be of continuing reference value. NASA counterpart of peer-reviewed formal professional papers but has less stringent limitations on manuscript length and extent of graphic presentations.

- TECHNICAL MEMORANDUM. Scientific and technical findings that are preliminary or of specialized interest, e.g., quick release reports, working papers, and bibliographies that contain minimal annotation. Does not contain extensive analysis.

- CONTRACTOR REPORT. Scientific and technical findings by NASA-sponsored contractors and grantees.

- CONFERENCE PUBLICATION. Collected papers from scientific and technical conferences, symposia, seminars, or other meetings sponsored or cosponsored by NASA.

- SPECIAL PUBLICATION. Scientific, technical, or historical information from NASA programs, projects, and missions, often concerned with subjects having substantial public interest.

- TECHNICAL TRANSLATION. English-language translations of foreign scientific and technical material pertinent to NASA's mission.

Specialized services also include creating custom thesauri, building customized databases, organizing and publishing research results.

For more information about the NASA STI program, see the following:

- Access the NASA STI program home page at *http://www.sti.nasa.gov*

- E-mail your question to *help@sti.nasa.gov*

- Fax your question to the NASA STI Information Desk at 443–757–5803

- Phone the NASA STI Information Desk at 443–757–5802

- Write to:
  STI Information Desk
  NASA Center for AeroSpace Information
  7115 Standard Drive
  Hanover, MD 21076–1320

NASA/TM—2013-216613

Comparison of Hyperthermal Ground Laboratory Atomic Oxygen Erosion Yields With Those in Low Earth Orbit

Bruce A. Banks
Science Application International Corporation, Cleveland, Ohio

Grace C. Dill and Ryan J. Loftus
Alphaport, Incorporated, Cleveland, Ohio

Kim K. de Groh and Sharon K. Miller
Glenn Research Center, Cleveland, Ohio

National Aeronautics and
Space Administration

Glenn Research Center
Cleveland, Ohio 44135

December 2013

Level of Review: This material has been technically reviewed by technical management.

Available from

NASA Center for Aerospace Information
7115 Standard Drive
Hanover, MD 21076–1320

National Technical Information Service
5301 Shawnee Road
Alexandria, VA 22312

Available electronically at http://www.sti.nasa.gov

Comparison of Hyperthermal Ground Laboratory Atomic Oxygen Erosion Yields With Those in Low Earth Orbit

Bruce A. Banks
Science Application International Corporation
Cleveland, Ohio 44135

Grace C. Dill and Ryan J. Loftus
Alphaport, Incorporated
Cleveland, Ohio 44135

Kim K. de Groh and Sharon K. Miller
National Aeronautics and Space Administration
Glenn Research Center
Cleveland, Ohio 44135

Abstract

The atomic oxygen erosion yields of 26 materials (all polymers except for pyrolytic graphite) were measured in two directed hyperthermal radio frequency (RF) plasma ashers operating at 30 or 35 kHz with air. The hyperthermal asher results were compared with thermal energy asher results and low Earth orbital (LEO) results from the Materials International Space Station Experiment 2 and 7 (MISSE 2 and 7) flight experiments. The hyperthermal testing was conducted to a significant portion of the atomic oxygen fluence similar polymers were exposed to during the MISSE 2 and 7 missions. Comparison of the hyperthermal asher prediction of LEO erosion yields with thermal energy asher erosion yields indicates that except for the fluorocarbon polymers of PTFE and FEP, the hyperthermal energy ashers are a much more reliable predictor of LEO erosion yield than thermal energy asher testing, by a factor of four.

1.0 Introduction

The reaction of low Earth orbital (LEO) atomic oxygen with hydrocarbon and halocarbon polymers has been a spacecraft durability concern for decades (Ref. 1). One of the most important characteristics of a polymer relating to its LEO durability is its atomic oxygen erosion yield which is the volume lost per incident atomic oxygen atom, given in cm^3/atom. The measurement of this value is most reliably performed by space experiments. However, because of the high cost, infrequent opportunity, and length of time to perform space experiments, ground laboratory systems have been developed which produce atomic oxygen in an effort to simulate the LEO environment. Due to the variety and complexity of the differences between the LEO atomic oxygen environment and ground laboratory simulations, differences exist which have not allowed the development of a simple relationship or proportionality between the LEO and ground laboratory erosion yields. Two of the most significant differences between most ground laboratory and LEO environments are the energy and directionality of the atomic oxygen.

A comparison between the erosion yields measured in an isotropic thermal energy (~0.04 eV) plasma asher and LEO directed hyperthermal (~4.5 eV) atomic oxygen was conducted using the results of the Materials International Space Station Experiment 2 (MISSE 2) (Refs. 2 and 3). These results indicated that the ratio of erosion yields relative to Kapton H polyimide were greater for 38 out of the 39 polymers tested in the thermal asher than in LEO. Testing has also been conducted with white Tedlar (TiO_2 pigment particle-filled polyvinylchloride) in LEO and in a directed hyperthermal energy asher (where the energy was greater than thermal energy but less than the sputter threshold of SiO_2 which is thought to be <20 eV). Results from exposure of white Tedlar indicated that the ratio of the erosion yield relative to Kapton H polyimide was less in the hyperthermal asher than in thermal energy ashers (Ref. 4). The

differences between the thermal energy and hyperthermal results is thought to be due to the directed versus isotropic nature of the arrival of atomic oxygen, differences in energy dependence of erosion yield, and presence of inorganic pigment particles causing better shielding from erosion in the case of directed hyperthermal attack.

The intent of this paper is to compare the results of directed hyperthermal asher erosion yields relative to Kapton H with those found from the results of the MISSE 2 and MISSE 7 experiments where the fluences were substantial enough (8.43×10^{21} and 4.18×10^{21} atoms/cm^2, respectively) to provide accurate erosion yields (Refs. 2 and 5).

2.0 Apparatus and Procedures

Two different directed hyperthermal RF plasma ashers, operating at different frequencies, were used to measure ground laboratory atomic oxygen erosion yields. The results were compared with erosion yields from isotropic thermal energy asher (13.56 MHz Structure Probe, Inc. Plasma Prep II) erosion yields (Ref. 3) and LEO flight data (Refs. 2 and 5). The two directed hyperthermal RF plasma ashers were a 35 kHz, LF-5 Axic plasma asher and a 30 kHz MCS, Model LF-6 plasma asher, both operated on air. Samples were placed in aluminum sample holders, which allowed exposure of a large central Kapton H sample and up to 21 smaller surrounding samples to simulate a portion of the MISSE 7 mission. The large central Kapton H fluence reference sample was 2.078 cm in diameter surrounded by up to 21 samples 0.886 cm in diameter as shown in Figure 1.

Two additional larger samples were also exposed in separate aluminum holders alongside the large sample holder plate in the 30 kHz hyperthermal asher as shown in Figure 2.

The flux within the hyperthermal ashers varies slightly with sample location in each asher. Thus, to estimate the fluence that each sample was exposed to, based on the fluence of the central large Kapton H sample, a flux calibration test was conducted in each asher with Kapton H samples in all the sample locations and operated for several days (72 hr in the 35 kHz asher and 70.2 hr in the 30 kHz asher). This allowed the computation of flux maps which were used to compute the relative fluence for all 22 or 24 sample positions for each asher based on the fluence of the central large Kapton H sample.

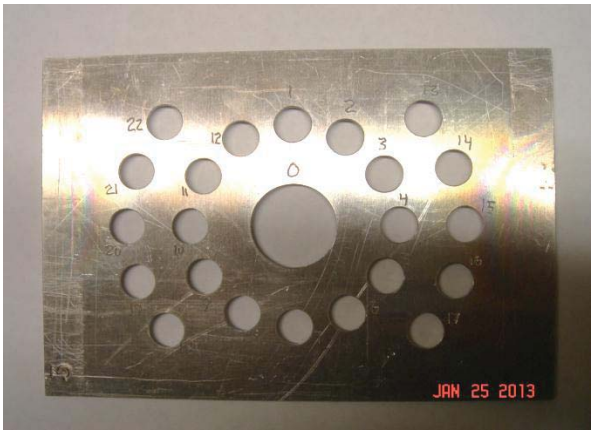

Figure 1.—Sample holder plate used in the 35 kHz hyperthermal asher.

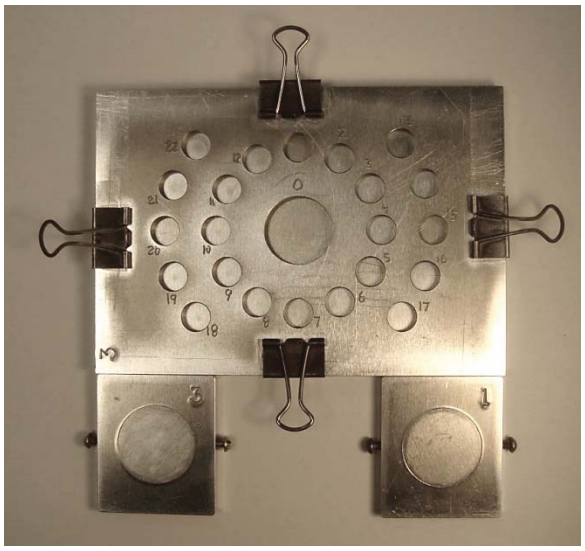

Figure 2.—Sample holders for hyperthermal atomic oxygen exposure simulating a portion of the materials flown on the MISSE-2 flight experiment in the 30 kHz hyperthermal asher.

The mass loss of 48 hr vacuum dehydrated Kapton H samples was used to obtain the Kapton H effective atomic oxygen fluence for the ground laboratory samples as described in ASTM E 2089-00 (Ref. 6) utilizing a Sartorius microgram balance. Based on the estimated erosion of the various polymers from both LEO and thermal energy asher testing, stacked layers of thin samples were used when possible to ensure that erosion all the way through the sample layers would be less likely to occur.

One of the goals of this investigation was to compare erosion yields more accurately by exposing samples to a significant Kapton H effective fluence as occurred in LEO. This approach was used because the erosion yields for most polymers that have significant ash content gradually diminishes with fluence due to shielding caused by the ash particles being exposed on the surfaces of the polymers (Refs. 4 and 7). In addition, multilayer samples tend to have higher erosion yields than single layer materials due to trapping of atomic oxygen as a layer becomes partially eroded (Ref. 8). To assure that the Kapton H effective fluence in the hyperthermal asher was a reasonably close simulation to the MISSE 2 and 7 fluences, the fluence on the central Kapton H sample was measured at approximately the half-fluence point of the MISSE 2 and 7 missions to allow for a midway correction to the exposure duration.

3.0 Results and Discussion

3.1 MISSE 7 Materials Simulation

The 72 hr atomic oxygen exposure of the sample plate to make a flux map for the MISSE 7 flight experiment resulted in a flux of 6.069×10^{15} atoms/(cm^2 sec) and a fluence of 1.573×10^{21} atoms/cm^2 on the large central Kapton H sample. The resulting ratio of flux at each sample location relative to the large central Kapton H sample is given in Table 1.

TABLE 1.—RATIO OF FLUX AT EACH SAMPLE LOCATION RELATIVE TO THE LARGE CENTRAL KAPTON H SAMPLE FOR THE 35 kHz ASHER FOR MATERIALS FLOWN ON THE MISSE 7 FLIGHT EXPERIMENT

Sample position	Flux relative to position 0
0	1.000
1	0.940
2	0.995
3	1.037
4	1.034
5	1.062
6	1.001
7	0.917
8	1.006
9	0.979
10	0.999
11	1.020
12	0.861
13	0.976
14	1.031
15	1.025
16	0.968
17	0.978
18	0.952
19	0.829
20	0.917
21	0.858
22	0.873

The results of a 190.3 hr exposure of most of the MISSE 7 materials in the 35 kHz directed hyperthermal asher are compared with LEO erosion yield results in Table 2.

The central Kapton H sample received a fluence of 3.51×10^{21}atoms/cm^2 which was 83.2 percent of the actual MISSE 7 experiment fluence. The uncertainties in the erosion yields are standard deviations computed using a propagation of error analysis as shown in Reference 9.

TABLE 2.—COMPARISON OF THE LEO AND DIRECTED HYPERTHERMAL 35 kHz ASHER EROSION YIELDS AND THEIR STANDARD DEVIATION UNCERTAINTIES FOR SIMULATION OF THE MISSE 7 ATOMIC OXYGEN EXPOSURE

Material	Abbrev.	Density, g/cm^3	Mass fraction of polymer that is ash (Ref. 7)	MISSE 7 erosion yield, cm^3/atom	35 Hz hyperthermal asher erosion yield, cm^3/atom	Ratio of 35 Hz hyperthermal asher to LEO erosion yield
White Tedlar	PVF	1.624	0.295	1.48±0.05 E-25	2.32±0.04 E-25	1.57
White Tedlar w/ 0.5 mil Kapton H cover	PVF	1.624	0.295	1.54±0.05 E-25	2.33±0.04 E-25	1.52
White Tedlar w/ 1.0 mil Kapton H cover	PVF	1.624	0.295	1.67±0.05 E-25	2.27±0.04 E-25	1.36
Kapton H	PI (H)	1.427	0.00284	3.00±0.03 E-24	3.00±0.03 E-24	1.00
Polyvinyl chloride	PVC	1.34	0.0033	1.74±0.03 E-24	5.15±0.03 E-24	2.96
Polyethylene	PE	0.918	0.0203	3.74±0.03 E-24	2.51±0.03 E-24	0.671
Polymethylpentene	PMP	0.833	<0.00043	4.45±0.03 E-24	3.12±0.03 E-24	0.700
Polyethersulfone	PES	1.37	0.0025	2.79±0.03 E-24	3.05±0.03 E-24	1.094
Aluminized-fluorinated ethylene propylene	Al-FEP	2.144	0.0668	1.81±0.03 E-25	3.90±0.03 E-24	21.548
Kapton HN	PI(HN)	1.435	0.00441	3.01±0.03 E-24	2.62±0.03 E-24	0.869
Kapton HN w/0.5 mil Kapton H cover	PI(HN)	1.435	0.00441	2.85±0.03 E-24	2.26±0.03 E-24	0.795
Kapton HN w/1.0 mil Kapton H cover	PI(HN)	1.435	0.00441	2.20±0.03 E-24	2.78±0.03 E-24	1.264
Polyamide-imide	Torlon	1.42	0.0234	1.74±0.03 E-24	2.74±0.03 E-24	1.574
Polyvinyl alcohol	PVOH	1.28	<0.000534	3.14±0.03 E-24	5.96±0.03 E-24	1.898
Cellulose Nitrate	CN	1.4	0.0020	7.34±0.06 E-24	8.29±0.06 E-24	1.130
Polyimide (AO resistant)	CORIN	1.36	0.1724	3.05±0.04 E-26	4.16±0.03 E-25	13.632
Urethane	LCP mesh	1.4	0.0782	4.61±0.06 E-25	3.28±0.06 E-25	0.712
Pyrolitic Graphite	PG	2.22	0.00154	4.15±0.45 E-25	4.05±0.03 E-25	0.976
Polytetrafluoroethylene	PTFE	2.1503	0.0427	1.42±0.04 E-25	6.98±0.03 E-24	49.218

3.2 MISSE 2 Materials Simulation

A 70.2 hr atomic oxygen exposure in the 30 kHz hyperthermal asher of the sample plate samples and two additional large samples all loaded with Kapton H was used to make a flux map for simulation of the MISSE 2 flight exposure. This resulted in an average flux of 2.73×10^{15} atoms/(cm^2 sec) and a fluence of 6.90×10^{20} atoms/cm^2 on the large central Kapton H sample. The fluence on the central Kapton H sample represents a fluence of 67.4 percent of the MISSE-2 fluence. The resulting ratio of flux at each sample location relative to the large central Kapton H sample is given in Table 3.

TABLE 3.—RATIO OF FLUX AT EACH SAMPLE LOCATION RELATIVE TO THE LARGE CENTRAL KAPTON H SAMPLE FOR THE 35 kHz ASHER FOR MATERIALS FLOWN ON THE MISSE 2 FLIGHT EXPERIMENT

Sample position	Flux relative to position 0
0	1.000
1	1.153
2	1.135
3	0.867
4	0.934
5	1.019
6	0.964
7	0.935
8	0.848
9	0.765
10	0.809
11	0.907
12	0.982
13	0.951
14	0.916
15	1.083
16	1.011
17	0.905
18	0.935
19	0.961
20	0.880
21	0.826
22	0.865
Large sample 1	0.935
Large sample 3	1.072

The erosion yield results from exposure of a portion of the MISSE-2 materials in the 30 kHz directed hyperthermal asher for 1284 hr are compared with LEO erosion yield results in Table 4.

TABLE 4.—COMPARISON OF THE LEO AND DIRECTED HYPERTHERMAL 30 kHz ASHER EROSION YIELDS AND THEIR STANDARD DEVIATION UNCERTAINTIES FOR SIMULATION OF THE MISSE 2 ATOMIC OXYGEN EXPOSURE

Material	Abbrev.	Density (g/cm^3) (Ref. 2)	Mass fraction of polymer that is ash (Ref. 7)	LEO erosion yield, cm^3/atom (Ref. 2)	30 kHz hyperthermal asher erosion yield, cm^3/atom	Ratio of 30 kHz hyperthermal asher to LEO erosion yield
Acrylonitrile butadiene styrene	ABS	1.05	0.0458	1.09±0.03 E-24	2.50±0.06 E-24	2.29
Cellulose acetate	CA	1.2911	0.00283	5.05±0.13 E-24	9.27±0.25 E-25	0.18
Poly-(p-phenylene terephthalamide)	PPDT	1.4422	0.00372	6.28±0.16 E-25	3.35±0.08 E-24	5.33
Polyethylene (low oxygen)	PE	0.918	0.0203	3.74±0.09 E-24	3.66±0.09 E-24	0.98
Polyvinyl fluoride	PVF	1.3792	0.00285	3.19±0.08 E-24	4.83±0.12 E-24	1.51
Crystalline polyvinylfluoride w/white pigment	PVF	1.6241	0.295	1.01±0.04 E-25	1.82±0.07 E-25	1.80
Polyoxymethylene; acetal; polyformaldehyde	POM	1.3984	0.00902	9.14±0.28 E-24	5.58±0.17 E-24	0.61
Polyacrylonitrile	PAN	1.1435	0.00184	1.41±0.05 E-24	3.41±0.11 E-24	2.42
Polystyrene	PS	1.0503	0.00042	3.74±0.10 E-24	3.65±0.10 E-24	0.98
Polymethyl methacrylate (Impact. Mod.)	PMMA	1.1628	0.00028	5.60±0.15 E-24	7.52±0.19 E-24	1.34
Polyethylene oxide	PEO	1.147	0.00112	1.93±0.05 E-24	1.39±0.04 E-23	7.19
Poly(p-phenylene-benzobisoxazole), balanced biaxial film	PBO	1.3976	0.0109	1.36±0.08 E-24	7.60±0.45 E-25	0.56
Epoxide or epoxy	EP	1.115	0.0304	4.21±0.11 E-24	5.04±0.14 E-24	1.20
Polypropylene	PP	0.9065	0.00184	2.68±0.07 E-24	6.85±0.18 E-24	2.56
Polybutylene terephthalate	PBT	1.3318	0.0629	9.11±0.24 E-25	2.10±0.05 E-24	2.30
Polysulfone	PSU	1.2199	0.00348	2.94±0.09 E-24	2.46±0.08 E-24	0.84
Polyeurethane	PU	1.2345	0.00664	1.56±0.05 E-24	1.98±0.06 E-24	1.27
Polyphenylene isophthalate	PPPA	0.72	0.0476	1.41±0.04 E-24	3.05±0.09 E-24	2.16
Pyrolytic Graphite	PG	2.22	0.00154	4.15±0.45 E-25	3.62±0.39 E-25	0.87
Polyetherimide	PEI	1.2873	0.00105	3.31±0.08E-24	2.74±0.07 E-24	0.83
Polyamide 6	PA 6	1.1233	0.00388	3.51±0.09 E-24	3.77±0.10 E-24	1.07
Polyamide 66	PA 66	1.2252	0.00459	1.80±0.23 E-24	3.65±0.46 E-24	2.03
Polyimide PMDA	PI (H)	1.4273	0.00284	3.00±0.07 E-24	3.00±0.07 E-24	1.00

3.3 Comparison Between 30 and 35 kHz Hyperthermal Ashers, Thermal Energy Asher, and LEO Results

A comparison of the erosion yields for two different hyperthermal ashers, a thermal energy asher, and the LEO environment is given in Table 5. The table only lists those materials that have been tested in multiple environments.

TABLE 5.—COMPARISON OF THE EROSION YIELDS FOR TWO DIFFERENT HYPERTHERMAL ASHERS, A THERMAL ENERGY ASHER, AND LEO

Material	Abbrev.	LEO erosion yield, cm^3/atom (Ref. 2)	Ratio of thermal energy asher erosion yield to LEO erosion yield (Ref. 3)	Ratio of 30 kHz hyperthermal asher erosion yield to LEO erosion yield	Ratio of 35 kHz hyperthermal asher erosion yield to LEO erosion yield
Acrylonitrile butadiene styrene	ABS	1.09 E-24	6.2	2.29	------
Cellulose acetate	CA	5.05 E-24	2.1	0.18	------
Poly-(p-phenylene terephthalamide)	PPDT	6.28 E-25	24.0	5.33	------
Polyethylene (low oxygen)	PE	3.74 E-24	1.8	0.98	0.671
Polyvinyl fluoride	PVF	3.19 E-24	1.6	1.51	
Crystalline polyvinylfluoride w/white pigment	PVF	1.01 E-25	37.1	1.80	1.57
Polyoxymethylene; acetal; polyformaldehyde	POM	9.14 E-24	2.8	0.61	------
Polyacrylonitrile	PAN	1.41 E-24	3.6	2.42	------
Polystyrene	PS	3.74 E-24	1.2	0.98	------
Polymethyl methacrylate (Impact. Mod.)	PMMA	5.60 E-24	1.9	1.34	------
Polyethylene oxide	PEO	1.93 E-24	9.3	7.19	------
Poly(p-phenylene-benzobisoxazole), balanced biaxial film	PBO	1.36 E-24	2.8	0.56	------
Epoxide or epoxy	EP	4.21 E-24	2.4	1.20	------
Polypropylene	PP	2.68 E-24	4.6	2.56	------
Polybutylene terephthalate	PBT	9.11 E-25	6.2	2.30	------
Polysulfone	PSU	2.94 E-24	1.3	0.84	------
Polyeurethane	PU	1.56 E-24	9.3	1.27	------
Polyphenylene isophthalate	PPPA	1.41 E-24	5.9	2.16	------
Pyrolytic Graphite	PG	4.15 E-25	1.2	0.87	0.976
Polyetherimide	PEI	3.31 E-24	1.2	0.83	------
Polyamide 6	PA 6	3.51 E-24	2.8	1.07	------
Polyamide 66	PA 66	1.80 E-24	4.7	2.03	------
Polyimide PMDA	PI (H)	3.00 E-24	1.0	1.00	1.00
Polyimide PMDA	PI (HN)	2.81 E-24	1.1	----	0.869
Fluorinated ethylene propylene	FEP	2.00 E-25	7.2	----	21.548
Polytetrafluoroethylene	PTFE	1.42 E-25	7.9	----	49.21
Averages			5.82	1.80	10.83
Averages excluding FEP and PTFE			5.67	1.80	1.02

The 30 kHz hyperthermal asher produced the closest average erosion yield approximation to LEO results. If one eliminates the fluorocarbon polymers FEP and PTFE, then the 35 kHz hyperthermal asher produces much closer erosion yield predictions to LEO results. The hyperthermal asher erosion yield of crystalline polyvinyl fluoride with white pigment particles is much closer to the LEO erosion yield values than the thermal energy asher value. This is thought to be due to the directed nature of the hyperthermal asher atomic oxygen which allows pigment particles to protect the underlying PVC matrix polymer (Refs. 7 and 10).

By averaging the ratio of all the hyperthermal asher erosion yields to the LEO values for each polymer (except for FEP and PTFE) and using Kapton H as a reference with an erosion yield of 3.00×10^{-24} cm^3/atom, then one can find a constant which allows one to estimate LEO erosion yield values based on hyperthermal or thermal energy asher erosion yields. Combining the data from the two hyperthermal energy ashers, the predicted LEO erosion yields averaged a factor of 0.256 times the values measured in the hyperthermal ashers. For thermal energy ashers, the predicted LEO erosion yields averaged a factor of 0.172 times the values measured in the thermal energy ashers. The magnitude of the ground laboratory-to-LEO proportional constants of 0.256 and 0.172 is not as important as the fractional variation between the predicted LEO erosion yields and the actual measured LEO erosion yields. If one compares the standard deviation of the ratio of predicted-to-measured atomic oxygen erosion yields for those materials that were tested in the two hyperthermal ashers and the thermal energy asher (Ref. 3), then an approximate determination can be made as to which type of asher is the most reliable predictor of LEO erosion yield as shown in Figure 3.

If one compares the hyperthermal energy atomic oxygen erosion yields to the LEO values, one would find that the LEO erosion yields, for the materials tested, are on the average lower (by a factor of 0.256) than the hyperthermal asher values. Thus, for some material of unknown erosion yield, the LEO erosion yield would be the hyperthermal energy asher measured erosion yield multiplied by 0.256 to obtain the estimate of the LEO value. Similarly, the LEO erosion yields predicted based on the thermal energy asher data need to be multiplied by 0.172 to obtain an estimate of the LEO values. However, some LEO erosion yield values will be higher or lower than the predictions. The fractional standard deviation in predicted erosion yield (predicted LEO erosion yield divided by measured LEO erosion yield) for all materials tested in the hyperthermal ashers was found to be 2.41, and for thermal energy asher predictions 1.37. Thus, using either type of asher, the fractional uncertainty in predicted LEO erosion yield is over 100 percent. However, if one excludes the fluoropolymers FEP and PTFE, then the fractional standard deviation in predicted erosion yield for the hyperthermal ashers was found to be only 0.375 and for thermal energy asher predictions 1.42.

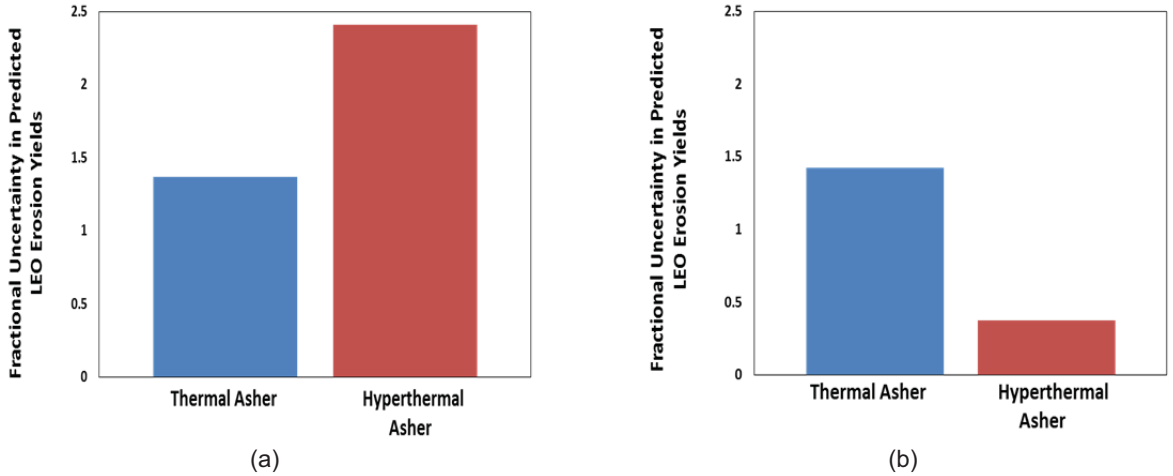

Figure 3.—Comparison of the fractional standard deviation uncertainty of the ratio of predicted erosion yields to LEO measured erosion yields: (a) all data, (b) all data excluding the results for FEP Teflon and PTFE.

Ideally, the most accurate prediction would be the lowest fractional uncertainty in the ratio of predicted-to-measured LEO erosion yields. As can be seen from Table 5 and Figure 3(a), the hyperthermal asher results for FEP and PTFE are more than an order of magnitude higher than all other polymers causing the hyperthermal asher to appear to be a poor predictor of LEO erosion yields. If one excludes FEP and PTFE results from the data, as shown in Figure 3(b), the hyperthermal asher appears to be a much more reliable (by a factor of ~3.8 better) predictor of LEO erosion yield than thermal energy asher testing. The reason why FEP and PTFE hyperthermal erosion yields are anomalous compared to the other polymers is not well understood.

The results indicate that the hyperthermal asher data (excluding FEP and PTFE) were able to predict the LEO erosion yields within a fractional standard deviation of ±37.5 percent whereas the thermal energy asher data predicted LEO results within ±142 percent. Thus, the prediction of LEO erosion yields can be estimated by multiplying the erosion yield measured in a hyperthermal asher by 0.256 to obtain an average uncertainty of ±37.5 percent. It should be pointed out that the erosion yield of most polymers is somewhat fluence and ash content dependent, thus, for significantly different fluences or ash fill contents, the predicted LEO erosion yields would be expected to be different.

4.0 Summary

The atomic oxygen erosion yields of 25 materials were measured in either of two directed hyperthermal RF plasma ashers operating at 30 and 35 kHz on air. The 30 kHz hyperthermal asher exposed 23 materials to ~5.69×10^{21} atoms/cm^2 representing a fluence of 67.4 percent of the MISSE 2 experiment and the 35 kHz hyperthermal asher exposed 19 materials to 3.51×10^{21}atoms/cm^2 which was 83.2 percent of the actual MISSE 7 experiment fluence. The direct comparison of hyperthermal erosion yield values to LEO values is somewhat compromised because of the difference in fluence between the asher and LEO exposures. This compromised comparison is due to the erosion yield of the polymers being somewhat dependent on fluence. This would be most compromising for the high ash content polymers. All the erosion yields were compared to LEO erosion yield values and for 26 of the materials, hyperthermal erosion yields were compared to thermal energy erosion yields.

Comparison of the hyperthermal asher prediction of LEO erosion yields with thermal energy asher erosion yields indicates that, except for the fluorocarbon polymers PTFE and FEP, the hyperthermal energy ashers are a much more reliable (by a factor of ~4 better) predictor of LEO erosion yield than thermal energy asher testing.

References

1. Leger, L.J., Spiker, I.K., Kuminecz, J.F., Ballentine, T.J., and Visentine, J.T., “STS Flight 5 LEO Effects Experiment - Background and Description of Thin Film Results,” AIAA-83-2631-CP, October, 1983.
2. de Groh, K.K., Banks, B.A., McCarthy, C.E., Rucker, R.N., Roberts, L.M. and Berger, L.A., “MISSE 2 PEACE Polymers Atomic Oxygen Erosion Experiment on the International Space Station,” Journal of High Performance Polymers 20 (2008) 388–409.
3. Stambler, A.H., Inoshita, K.E., Roberts, L.M., Barbagallo, C.E., de Groh, K.K., Banks, B.A., “Ground-Laboratory to In-Space Atomic Oxygen Correlation for the PEACE Polymers,” Proceedings of the 9th International Conference on Protection of Materials and Structures from Space Environment,” (conference held May 19–23, 2008 in Toronto, Canada) Ed. J.I. Kleiman, AIP Conference Proceedings 1087, pp. 51–66, 2009; also NASA/TM—2011-126904.
4. Banks, B.A., Simmons, J.C., de Groh, K.K., Miller, S.K., “The Effect of Ash and Inorganic Pigment Fill on the Atomic Oxygen Erosion of Polymers and Paints,” Proceedings of the 12th International Symposium on Materials in the Space Environment (ISMSE 12), Noordwijk, The Netherlands (ESA SP-705, February 2013).

5. Yi, G.T., de Groh, K.K. Banks, B.A., Haloua, A., Imka, E.C., and Mitchell, G.G., "Overview of the MISSE 7 Polymers and Zenith Polymers Experiments After 1.5 Years of Space Exposure," Proceedings of the "12th International Symposium on Materials in the Space Environment (ISMSE 12)," Noordwijk, The Netherlands (ESA SP-705, February 2013); also NASA/TM—2013-217848, 2013.
6. ASTM E 2089-00, "Standard Practices for Ground Laboratory Atomic Oxygen Interaction Evaluation of Materials for Space Applications," June 2000.
7. Banks, B.A., Simmons, J.C., de Groh, K.K., Miller, S.K., "The Effect of Ash and Inorganic Pigment Fill on the Atomic Oxygen Erosion of Polymers and Paints," Proceedings of the "12th International Symposium on Materials in the Space Environment (ISMSE 12)," Noordwijk, The Netherlands (ESA SP-705, February 2013).
8. de Groh, K.K., Banks, B.B., Mitchell, G.G., Yi, G.T., Guo, A., Ashmead, C.C., Roberts, L.M., McCarthy, C.E. and Sechkar, E.A., "MISSE 6 Stressed Polymers Experiment Atomic Oxygen Erosion Data," Proceedings of Proceedings of the "12th International Symposium on Materials in the Space Environment (ISMSE 12)," Noordwijk, The Netherlands (ESA SP-705, February 2013).
9. McCarthy, C.E., Banks, B.A., and de Groh, K.K., Miller, S.K., "MISSE 2 PEACE Polymers Experiment Atomic Oxygen Erosion Yield Error Analysis," NASA/TM—2010-216903, Nov. 2010.
10. Banks, B.A., Bacus, J.A., Manno, M.V., Waters, D.L., Cameron, K.C., and de Groh, K.K., "Prediction of Atomic Oxygen Erosion Yield for Spacecraft Polymers," Volume 48, Number 1, Journal of Spacecraft and Rockets, Jan./Feb. 2011.